

2

TECHNICAL REPORT BRL-TR-3092

AD-A221 710

**BRL**

ON THE SPATIAL EIGENVALUE APPROACH  
TO HIGH REYNOLDS NUMBER FLOW IN  
A ROTATING AND NUTATING CYLINDER

PHILIP HALL  
RAYMOND SEDNEY  
NATHAN GERBER

APRIL 1990

DTIC  
ELECTE  
MAY 21 1990  
S B D

APPROVED FOR PUBLIC RELEASE; DISTRIBUTION UNLIMITED.

U.S. ARMY LABORATORY COMMAND

BALLISTIC RESEARCH LABORATORY  
ABERDEEN PROVING GROUND, MARYLAND

## NOTICES

Destroy this report when it is no longer needed. DO NOT return it to the originator.

Additional copies of this report may be obtained from the National Technical Information Service, U.S. Department of Commerce, 5285 Port Royal Road, Springfield, VA 22161.

The findings of this report are not to be construed as an official Department of the Army position, unless so designated by other authorized documents.

The use of trade names or manufacturers' names in this report does not constitute indorsement of any commercial product.

**REPORT DOCUMENTATION PAGE**Form Approved  
OMB No. 0704-0188

Public reporting burden for this collection of information is estimated to average 1 hour per response, including the time for reviewing instructions, searching existing data sources, gathering and maintaining the data needed, and completing and reviewing the collection of information. Send comments regarding this burden estimate or any other aspect of this collection of information, including suggestions for reducing this burden, to Washington Headquarters Services, Directorate for Information Operations and Reports, 1215 Jefferson Davis Highway, Suite 1204, Arlington, VA 22202-4302, and to the Office of Management and Budget, Paperwork Reduction Project (0704-0188), Washington, DC 20503.

**1. AGENCY USE ONLY (Leave blank)****2. REPORT DATE**

April 1990

**3. REPORT TYPE AND DATES COVERED**

Technical, Nov 87 - Nov 89

**4. TITLE AND SUBTITLE**

On the Spatial Eigenvalue Approach to High Reynolds Number Flow in a Rotating and Nutating Cylinder

**5. FUNDING NUMBERS**

PE: 62618A

PR: 1L1 62618AH80

**6. AUTHOR(S)**

Hall\*, Philip, Sedney, Raymond and Gerber, Nathan

**7. PERFORMING ORGANIZATION NAME(S) AND ADDRESS(ES)**US Army Ballistic Research Laboratory  
ATTN: SLCBR-LF  
Aberdeen Proving Ground, MD 21005-5066**8. PERFORMING ORGANIZATION  
REPORT NUMBER**

BRL-TR-3092

**9. SPONSORING / MONITORING AGENCY NAME(S) AND ADDRESS(ES)**US Army Ballistic Research Laboratory  
ATTN: SLCBR-DD-T  
Aberdeen Proving Ground, MD 21005-5066**10. SPONSORING / MONITORING  
AGENCY REPORT NUMBER****11. SUPPLEMENTARY NOTES**

\*University of Exeter, Exeter, England and ICASE, Hampton, Virginia

**12a. DISTRIBUTION / AVAILABILITY STATEMENT**

Approved for public release; distribution unlimited.

**12b. DISTRIBUTION CODE****13. ABSTRACT (Maximum 200 words)**

The spatial eigenvalue expansion procedure which we have used previously to study viscous flow in rotating and nutating cylinders is studied in the high Reynolds number limit. It is shown that in this limit there is a significant simplification in the procedure used to determine the amplitudes of the eigenfunctions used to describe the forced velocity field in the cylinder. More precisely, it is shown that these amplitudes can, to the order of Reynolds number used in this paper, be simply expressed in terms of Bessel functions. The method is used to calculate the pressure coefficient at a point on the endwall. Detailed comparisons with experimental results are made. It is found that the approach provides an accurate and extremely rapid way of determining this pressure coefficient.

**14. SUBJECT TERMS**High Reynolds number; Liquid-filled projectile; Pressure coefficient; Rotating Fluid;  
Rotating nutating cylinder; Spatial eigenvalues**15. NUMBER OF PAGES**

41

**16. PRICE CODE****17. SECURITY CLASSIFICATION  
OF REPORT**

UNCLASSIFIED

**18. SECURITY CLASSIFICATION  
OF THIS PAGE**

UNCLASSIFIED

**19. SECURITY CLASSIFICATION  
OF ABSTRACT**

UNCLASSIFIED

**20. LIMITATION OF ABSTRACT**

SAR

## GENERAL INSTRUCTIONS FOR COMPLETING SF 298

The Report Documentation Page (RDP) is used in announcing and cataloging reports. It is important that this information be consistent with the rest of the report, particularly the cover and title page. Instructions for filling in each block of the form follow. It is important to *stay within the lines* to meet optical scanning requirements.

**Block 1. Agency Use Only (Leave blank).**

**Block 2. Report Date.** Full publication date including day, month, and year, if available (e.g. 1 Jan 88). Must cite at least the year.

**Block 3. Type of Report and Dates Covered**  
State whether report is interim, final, etc. If applicable, enter inclusive report dates (e.g. 10 Jun 87 - 30 Jun 88).

**Block 4. Title and Subtitle.** A title is taken from the part of the report that provides the most meaningful and complete information. When a report is prepared in more than one volume, repeat the primary title, add volume number, and include subtitle for the specific volume. On classified documents enter the title classification in parentheses.

**Block 5. Funding Numbers.** To include contract and grant numbers; may include program element number(s), project number(s), task number(s), and work unit number(s). Use the following labels:

C - Contract	PR - Project
G - Grant	TA - Task
PE - Program Element	WU - Work Unit Accession No.

**Block 6. Author(s)** Name(s) of person(s) responsible for writing the report, performing the research, or credited with the content of the report. If editor or compiler, this should follow the name(s).

**Block 7. Performing Organization Name(s) and Address(es).** Self-explanatory.

**Block 8. Performing Organization Report Number.** Enter the unique alphanumeric report number(s) assigned by the organization performing the report.

**Block 9. Sponsoring/Monitoring Agency Name(s) and Address(es)** Self-explanatory.

**Block 10. Sponsoring/Monitoring Agency Report Number.** (If known)

**Block 11. Supplementary Notes.** Enter information not included elsewhere such as: Prepared in cooperation with...; Trans. of...; To be published in.... When a report is revised, include a statement whether the new report supersedes or supplements the older report.

**Block 12a. Distribution/Availability Statement.** Denotes public availability or limitations. Cite any availability to the public. Enter additional limitations or special markings in all capitals (e.g. NOFORN, REL, ITAR).

DOD - See DoDD 5230.24, "Distribution Statements on Technical Documents."

DOE - See authorities.

NASA - See Handbook NHB 2200.2.

NTIS - Leave blank.

**Block 12b. Distribution Code.**

DOD - Leave blank.

DOE - Enter DOE distribution categories from the Standard Distribution for Unclassified Scientific and Technical Reports.

NASA - Leave blank.

NTIS - Leave blank.

**Block 13. Abstract.** Include a brief (Maximum 200 words) factual summary of the most significant information contained in the report.

**Block 14. Subject Terms.** Keywords or phrases identifying major subjects in the report.

**Block 15. Number of Pages.** Enter the total number of pages.

**Block 16. Price Code.** Enter appropriate price code (NTIS only).

**Blocks 17. - 19. Security Classifications.** Self-explanatory. Enter U.S. Security Classification in accordance with U.S. Security Regulations (i.e., UNCLASSIFIED). If form contains classified information, stamp classification on the top and bottom of the page.

**Block 20. Limitation of Abstract.** This block must be completed to assign a limitation to the abstract. Enter either UL (unlimited) or SAR (same as report). An entry in this block is necessary if the abstract is to be limited. If blank, the abstract is assumed to be unlimited.

# TABLE OF CONTENTS

	<u>Page</u>
List of Figures	v
1. Introduction and formulation	1
2. The spatial eigenvalue approach in the limit $Re \rightarrow \infty$	4
The pressure coefficient	9
3. Results and discussion	14
References	27



Accession For	
NTIS GRA&I	<input checked="" type="checkbox"/>
DTIC TAB	<input type="checkbox"/>
Unannounced	<input type="checkbox"/>
Justification	
By _____	
Distribution/	
Availability Codes	
Dist	Avail and/or Special
A-1	

INTENTIONALLY LEFT BLANK.

# LIST OF FIGURES

<u>Figure</u>		<u>Page</u>
1	The first 72 eigenvalues for $Re = 1000, f = 0.1$ (taken from Reference 2).....	16
2	The eigenvalue spectrum for some large values of $Re$ and $f = 0.08$ .....	17
3a	The behavior of $c_p$ calculated using the composite expansion with $A = 3.1481, Re = 5000$ . The experimental points are from Reference 7.....	18
3b	The behavior of $c_p$ calculated using the composite expansion with $A = 3.1481, Re = 100,000$ .....	19
3c	The behavior of $c_p$ calculated using the composite expansion with $A = 3.1481, Re = 500,000$ .....	20
4a	The behavior of $c_p$ calculated using the composite expansion with $A = 1.0509, Re = 100,000$ .....	21
4b	The behavior of $c_p$ calculated using the composite expansion with $A = 1.0509, Re = 500,00$ .....	22
5	Variation of the frequency of peak response with $Re$ for $A = 3.148$ . Solid line is from the approach of Reference 4. The crosses are from the present calculations.....	23
6a	A 3D plot of $c_p$ against $A$ and $f$ for the case $Re = 100,000$ .	24
6b	A 3D plot of $c_p$ against $A$ and $f$ for the case $Re = 500,000$ .	25

INTENTIONALLY LEFT BLANK.

## 1. Introduction and formulation

It is well-known that there can be a significant difference in behavior in flight between liquid-filled and solid-filled projectiles. The difference is caused by the motion of the liquid inside the spinning projectile. This motion causes forces to act on the projectile which can ultimately cause the flight of the projectile to be prematurely terminated by instability. The initial motion of the projectile necessarily causes the fluid motion in the cylinder to be time-dependent; later it can be assumed that the flow is steady. It is the latter situation which is investigated here.

Our concern then is with the motion of an incompressible viscous fluid of kinematic viscosity  $\nu$  in a cylinder of length  $2Aa$  and radius  $a$ . The cylinder is spinning at a constant rate about its axis, which, in turn, is nutating at a constant rate and yaw angle about an axis directed along its trajectory. Throughout this calculation  $a$  will be used as an appropriate length scale while the magnitude of a typical velocity is taken to be  $(\Omega + \bar{\tau} \cos K_0)a$ , where  $\Omega$  is the magnitude of the angular velocity of the projectile as observed in the aeroballistic reference frame,  $\bar{\tau}$  is the dimensional coning frequency, and  $K_0$  is the coning angle. (In the aeroballistic frame, one cartesian coordinate lies along the cylinder axis and a second coordinate lies in the plane of the cylinder axis and trajectory; see, e.g., Reference 1).  $K_0$  is assumed small throughout this work, so that it is possible to determine the properties of the forced motion using a simple perturbation expansion in powers of  $K_0$ . We nondimensionalize the coning frequency as follows:

$$\tau = \frac{\bar{\tau}}{(\Omega + \bar{\tau} \cos K_0)} \quad (1.1)$$

and we define the Reynolds number by

$$Re = \frac{(\Omega + \bar{\tau} \cos K_0)a^2}{\nu} \quad (1.2)$$

By use of the assumption already introduced,  $K_0 \ll 1$ ,  $\cos K_0$  is replaced by unity in the above and in the following. The typical time, length, velocity, and pressure scales used to nondimensionalize the flow variables are  $(\Omega + \bar{\tau})^{-1}$ ,  $a$ ,  $(\Omega + \bar{\tau})a$ , and  $\rho a^2(\Omega + \bar{\tau})^2$ , where  $\rho$  is the density of the fluid.

In a previous paper, Hall et al.<sup>[2]</sup>, hereafter referred to as HSG, we used the spatial eigenvalue approach to determine the forced motion in the projectile at finite values of the Reynolds number. Here we aim to extend the results of HSG to the high Reynolds number limit and show that in this case there is a significant simplification of the problem. We now indicate how the appropriate partial differential system to be solved can be derived

from the Navier-Stokes equations of motion. Our derivation is of course only brief so the reader is referred to HSG and the references therein for a more complete account.

First the Navier-Stokes equations are written down with respect to an inertial cylindrical polar co-ordinate system  $(r, \theta, x)$  with corresponding velocity components  $(u, v, w)$  and pressure  $p$ . The coning motion of the projectile means that the boundary conditions must be applied at a moving surface; this is the main drawback in the use of the inertial reference frame but for small angles a Taylor series expansion of the different flow quantities about the mean position of the cylinder produces boundary conditions at a fixed surface. Thus it is assumed that the motion of the cylinder is proportional to  $\exp i\{ft - \theta\}$  where  $t$  denotes nondimensional time and  $f$  is, in general, the nondimensional complex frequency of the projectile motion. We shall take  $f$  to be real so that

$$f = \tau. \quad (1.3)$$

Since  $K_0$ , the coning angle, has been assumed small we expect only small departures from solid body rotation and the velocity components are therefore  $(-K_0 u^*, r - K_0 v^*, -K_0 w^*)$  and the pressure is  $\frac{1}{2}r^2 - K_0 p^*$ . Here a star denotes a perturbation quantity.

It is assumed in our calculation that the motion of the cylinder is specified; we do not allow for a feedback from the fluid to the projectile. Following HSG it is convenient to define complex velocities and pressures, denoted by underlining and given by

$$(u^*, v^*, w^*, p^*) = \text{Real}\{(\underline{u}, \underline{v}, \underline{w}, \underline{p}) \exp i\{ft - \theta\}\}. \quad (1.4)$$

The resulting nondimensional Navier-Stokes equations are

$$\begin{aligned} i(f-1)\underline{u} - 2\underline{v} &= -\underline{p}_r + Re^{-1}[\nabla^2 \underline{u} - \frac{2}{r^2}\underline{u} + \frac{2i}{r^2}\underline{v}], \\ i(f-1)\underline{v} + 2\underline{u} &= (i/r)\underline{p} + Re^{-1}[\nabla^2 \underline{v} - \frac{2}{r^2}\underline{v} - \frac{2i}{r^2}\underline{u}], \\ i(f-1)\underline{w} &= -\underline{p}_x + Re^{-1}[\nabla^2 \underline{w} - \frac{1}{r^2}\underline{w}], \\ (r\underline{u})_r - i\underline{v} + r\underline{w}_x &= 0, \end{aligned}$$

where  $\nabla^2 = \partial_r^2 + \frac{1}{r}\partial_r + \partial_x^2$  and subscripts denote partial derivatives.

We now choose to seek separable solutions of these equations which take the form

$$(\underline{u}, \underline{v}, \underline{w}, \underline{p}) = (U(r) \sin Kx, V(r) \sin Kx, W(r) \cos Kx, P(r) \sin Kx), \quad (1.5)$$

and in this case it follows that  $(U, V, W, P)$  satisfies

$$\begin{aligned} [Re^{-1}(\nabla_1 - r^{-2}) - iM]U + 2[1 + (i/r^2 Re)]V - P_r &= 0 \\ [Re^{-1}(\nabla_1 - r^{-2}) - iM]V - 2[1 + (i/r^2 Re)]U + \frac{iP}{r} &= 0 \\ [Re^{-1}\nabla_1 - iM]W - KP &= 0 \\ (rU)_r - iV - KrW &= 0. \end{aligned} \quad (1.6a, b, c, d)$$

where  $M = f - 1$

and  $\nabla_1 \equiv d_{rr} + \frac{1}{r}d_r - [\frac{1}{r^2} + K^2]$ .

These equations must be solved subject to an inhomogeneous condition at  $r = 1$  and an appropriate condition at  $r = 0$ . We obtain

$$U - iV = W = P = 0, \quad r = 0 \quad (1.7)$$

at the centre of the cylinder. For a discussion of the origin of (1.7) the reader is referred to Batchelor and Gill<sup>[3]</sup>. The ordinary differential system specified by (1.6), (1.7) and the no-slip condition at the cylinder constitutes an eigenvalue problem

$$K = K(Re, f). \quad (1.8)$$

At finite values of  $Re$  there are no real solutions of that eigenvalue problem so that solid body rotation is stable to the first non-axisymmetric Taylor vortex mode of instability. At infinite values of  $Re$  solid body rotation is, according to Rayleigh's criterion, neutrally stable and this is the origin of the real values of  $K$  which that eigenvalue problem has in the limit  $Re \rightarrow \infty$ . We restrict our attention to the case when the pivot point for the cylinder is midway along its axis. From Gerber et al.<sup>[4]</sup> we know that the forced problem at small amplitudes then leads to the following conditions for  $\underline{u}$ ,  $\underline{v}$  and  $\underline{w}$  at the walls:

$$\begin{aligned} \underline{u} &= -i(1 - f)x, \\ \underline{v} &= -(1 - f)x, \\ \underline{w} &= i(1 - f)r. \end{aligned} \quad (1.9a, b, c)$$

Following HSG we transfer the inhomogeneous boundary conditions to the endwall by writing

$$\begin{aligned} \underline{u} &= -i[1 - f]x + u(r, x), \\ \underline{v} &= -[1 - f]x + v(r, x), \\ \underline{w} &= i[1 - f]r + \phi(r) + w(r, x), \\ \underline{p} &= -[1 - f^2]rx + p(r, x), \\ \phi(r) &= 2if \left[ r - \frac{J_1(\lambda r)}{J_1(\lambda)} \right]. \end{aligned} \quad (1.10a, b, c, d, e)$$

Here  $J_1$  denotes the order 1 Bessel function of the first type while  $\lambda$  is defined by

$$\lambda = (1 + i)\sqrt{(1 - f)Re/2}. \quad (1.11)$$

Since we will be interested in the limit of high Reynolds numbers we can drop the Bessel function terms in (1.10) away from  $r = 1$ . We note in passing here that  $\lambda$ , and hence  $u$  etc. have a branch cut at  $f = 1$ ; we will not investigate such high frequencies here since the ballistic applications of our work typically correspond to values of  $f$  less than .5. In a separate study eigenvalues and the pressure coefficient  $c_p$  were calculated for  $1 < f \leq 1.5$ . The results were to be compared with experimental data for  $f > 1$ . In terms of  $u, v, w$  and  $p$  it follows from above that the appropriate boundary conditions are

$$\begin{aligned} u - iv = w = p = 0, \quad r = 0 \\ u = v = w = 0, \quad r = 1 \\ u = v = 0, w = -\phi(r) \quad x = \pm A. \end{aligned} \quad (1.12a, b, c)$$

Furthermore, we note that  $u, v, w, p$  satisfy (1.5) and (1.6) and following the spatial eigenvalue approach of HSG we therefore write

$$\begin{aligned} u = \sum_{n=1}^{\infty} \frac{\alpha_n \sin k_n x}{\sin k_n A} u_n(r), \quad v = \sum_{n=1}^{\infty} \frac{\alpha_n \sin k_n x}{\sin k_n A} v_n(r), \\ w = \sum_{n=1}^{\infty} \frac{\alpha_n \cos k_n x}{\sin k_n A} w_n(r), \quad p = \sum_{n=1}^{\infty} \frac{\alpha_n \sin k_n x}{\sin k_n A} p_n(r). \end{aligned} \quad (1.13a, b, c, d)$$

Here  $\{k_n\}$  is the infinite sequence of eigenvalues of (1.6), (1.7) and the coefficients  $\{\alpha_n\}$  are to be determined. In HSG these constants were found by collocation at the endwalls; here we shall make the further limit  $Re \rightarrow \infty$  and show how asymptotic expressions for these coefficients can be found.

## 2. The spatial eigenvalue approach in the limit $Re \rightarrow \infty$ .

On the basis of our experience with the eigenvalue problem for  $\{k_n\}$  at finite values of  $Re$  we know that the eigenvalues split into groups of three which can be ordered by, for example, connecting them to the eigenvalues of a related Taylor vortex problem. We anticipate this split and therefore consider the three sets of eigenvalues  $\{k_{j,n}\}$ , for  $j = 1, 2, 3$  and  $n = 1, 2, 3, \dots$ . The distribution of eigenvalues is illustrated in Figure 1 for the case  $Re = 1000$  and  $f = .1$ ; this is taken from HSG wherein the labeling of the eigenvalues is discussed. (Note that the eigenvalue  $k_{3,1}$  was labeled on the basis of an analysis pertinent to the limit  $Re \rightarrow 0$ . However, in the limit  $Re \rightarrow \infty$ , it lies in the set of values determined

by Stewartson's analysis<sup>[5]</sup>.) In Figure 2 we show the development of the spectrum as  $Re$  increases, for fixed  $f$  and  $j = 1$ . We note that for sufficiently small  $n$  the eigenvalues approach the real axis while for large  $n$  the eigenvalues approach the imaginary axis.

On the other hand numerical calculations in HSG showed that the  $j = 2, 3$  branches had  $|k_{jn}| \sim Re^{\frac{1}{2}}$  for  $Re \gg 1$ . We shall now describe the precise details of the asymptotic structure of  $\{k_{jn}\}$  for  $j = 1, 2, 3$  in the limit  $Re \rightarrow \infty$  and hence put ourselves into a position to find asymptotic forms for  $\{\alpha_n\}$ . Splitting of the eigenvalues into triplets leads naturally to the definitions of branches 1, 2 and 3 in the complex  $k$  plane for  $j = 1, 2, 3$  respectively. The corresponding amplitude functions are denoted by  $\epsilon_n, \gamma_n$  and  $\beta_n$ , replacing the  $\alpha_n$ .

First we derive the asymptotic structure of the  $j = 1$  modes; the analysis is, of course, essentially inviscid and based on that given by Stewartson<sup>[5]</sup>. We seek an asymptotic solution for the  $n^{th}$  eigenvalue  $k_{1n}$  by writing

$$k_{1n} = k_{1n}^0 + k_{1n}^1 Re^{-\frac{1}{2}} + k_{1n}^2 Re^{-1} + \dots, \quad (2.1)$$

while

$$u_{1n} = u_{1n}^0 + u_{1n}^1 Re^{-\frac{1}{2}} + u_{1n}^2 Re^{-1} + \dots, \quad (2.2)$$

together with similar expansions for  $v_{1n}, w_{1n}$  and  $p_{1n}$ . If we define  $\sigma$  by

$$\sigma = i\{f - 1\}$$

then substitution of (2.1), (2.2) into (1.6) with  $K$  replaced by  $k_{1n}$  yields a system of equations for  $u_{1n}^0, v_{1n}^0, w_{1n}^0, p_{1n}^0$  which has the solution

$$\begin{aligned} \{\sigma^2 + 4\}u_{1n}^0 &= i \left\{ (1-f)\mu_{1n}^0 J_1'(\mu_{1n}^0 r) + \frac{2J_1(\mu_{1n}^0 r)}{r} \right\}, \\ \{\sigma^2 + 4\}v_{1n}^0 &= \left\{ (1-f)\frac{J_1(\mu_{1n}^0 r)}{r} + 2\mu_{1n}^0 J_1'(\mu_{1n}^0 r) \right\}, \\ w_{1n}^0 &= \frac{-k_{1n}^0}{\sigma} J_1(\mu_{1n}^0 r), \\ p_{1n}^0 &= J_1(\mu_{1n}^0 r). \end{aligned} \quad (2.3a, b, c, d)$$

$$(\mu_{1n}^0)^2 = (k_{1n}^0)^2 \frac{(3-f)(1+f)}{(1-f)^2}. \quad (2.4)$$

The radial velocity component above satisfies the sidewall condition if

$$(1-f)\mu_{1n}^0 J_1'(\mu_{1n}^0) + 2J_1(\mu_{1n}^0) = 0 \quad (2.5)$$

which has an infinite number of eigenvalues on the positive real axis. [Information on this spectrum can be found in 'Conduction of Heat in Solids' by H.S. Carslaw and J.C. Jaeger, Oxford University Press, 1947.] The eigenvalues with  $j = 1$  become progressively closer to the real axis in the limit  $Re \rightarrow \infty$ . The Stewartson eigenvalues correspond to a choice of frequency such that  $k_{1n}^0 A = \frac{\pi}{2} \{1 + N\}$  for  $N$  an even non-negative integer. Thus, at the resonant frequencies of a cylinder of given length, the  $j = 1$  eigenvalues approach Stewartson's eigenvalues. Since we have not retained viscous effects in the perturbation equations, we can, of course, only make the radial velocity component vanish at  $r = 1$ . The other velocity components must therefore be reduced to zero within a boundary layer of thickness  $Re^{-\frac{1}{2}}$  near  $r = 1$ . The determination of the velocity field within this layer will enable us to determine the order  $Re^{-\frac{1}{2}}$  term in (2.1), we shall give some of the detail necessary to determine it.

First we note that the perturbation equations for  $r = 0(1)$  proceed in powers of  $Re$  so that if we define  $\mu_{1n}$  by

$$\mu_{1n} = \mu_{1n}^0 + \mu_{1n}^1 Re^{-\frac{1}{2}} + \dots, \quad (2.6)$$

then correct to order  $Re^{-\frac{1}{2}}$ , (2.3) are valid if  $u_{1n}^0, v_{1n}^0, w_{1n}^0, p_{1n}^0$  and  $\mu_{1n}^0$  are replaced by  $u_{1n}^0 + u_{1n}^1 Re^{-\frac{1}{2}}$ , etc. and then

$$\mu_{1n}^0 \mu_{1n}^1 = k_{1n}^0 k_{1n}^1 \frac{(3-f)(1+f)}{(1-f)^2}. \quad (2.7)$$

It follows that when  $r \rightarrow 1$

$$(3-f)(1+f)u_{1n}^1 \rightarrow -\mu_{1n}^1 i \left\{ \mu_{1n}^0 J_1(\mu_{1n}^0)(1-f) \left[ 1 + \frac{(3-f)(1+f)}{(\mu_{1n}^0)^2(1-f)^2} \right] \right\} + C\zeta, \quad (2.8)$$

where  $\zeta = Re^{\frac{1}{2}}(1-r)$ , and  $C$  is a constant to be determined later. In the boundary layer at  $r = 1$  we write

$$Re^{\frac{1}{2}}u_{1n} = \tilde{u}_{1n}^0 + \tilde{u}_{1n}^1 Re^{-\frac{1}{2}} + \dots$$

together with similar expansions for  $v_{1n}, w_{1n}$ , and  $p_{1n}$ . It can be shown that the zeroth order system obtained by substituting these expansions into (1.6) written in terms of  $\zeta$  yields

$$\tilde{p}_{1n}^0 = \text{constant}, \quad \tilde{u}_{1n}^0 = \left\{ \frac{ip_{1n}^0}{1-f} \right\} \left\{ 1 + (k_{1n}^0)^2 \right\} \left\{ \frac{1}{\sqrt{\sigma}} e^{-\sqrt{\sigma}\zeta} - \frac{1}{\sqrt{\sigma}} + \zeta \right\}$$

when solved subject to  $\tilde{u}_{1n}^0 = \tilde{v}_{1n}^0 = \tilde{w}_{1n}^0 = 0$ ,  $\zeta = 0$ . Thus matching the pressure and radial velocity component when the inviscid and viscous regions meet give

$$\tilde{p}_{1n}^0 = J_1(\mu_{1n}^0), \quad \frac{iJ_1(\mu_{1n}^0)[1 + (k_{1n}^0)^2]}{(1-f)\sigma^{\frac{1}{2}}} = \frac{i\mu_{1n}^0 J_1(\mu_{1n}^0)(1-f)\mu_{1n}^1}{(3-f)(1+f)} \left\{ 1 + \frac{(3-f)(1+f)}{(\mu_{1n}^0)^2(1-f)^2} \right\},$$

and an expression for  $C$  the constant in (2.8). Using (2.7) and the eigenrelation (2.5) the second of the above equations can be manipulated to give

$$k_{1n} = k_{1n}^0 \left\{ 1 + \frac{1+i}{\sqrt{1-f}\sqrt{2Re}} + \dots \right\} \quad (2.9)$$

where  $k_{1n}^0$  is determined by (2.4) and (2.5).

The viscous modes have an  $x$ -dependence on a  $Re^{-\frac{1}{2}}$  lengthscale. For convenience we drop the '2n' and '3n' notation for the moment and seek a viscous eigenvalue of (1.6) and (1.7) by writing

$$k = \sqrt{Re} k_0 + \frac{1}{\sqrt{Re}} k_1 + \dots \quad (2.10)$$

while  $u, v, w$ , and  $p$  expand as

$$\begin{aligned} u &= u_0 + \frac{1}{\sqrt{Re}} u_1 + \dots, \\ v &= v_0 + \frac{1}{Re^{\frac{1}{2}}} v_1 + \dots, \\ w &= \frac{w_0}{\sqrt{Re}} + \frac{w_1}{Re} + \dots, \\ p &= \frac{p_0}{Re} + \frac{p_1}{Re^{\frac{3}{2}}} + \dots. \end{aligned} \quad (2.11a, b, c, d)$$

The zeroth order approximation to (1.6) then yields

$$\begin{aligned} \{-k_0^2 - if + i\}u_0 + 2v_0 &= 0, \\ \{-k_0^2 - if + i\}v_0 - 2u_0 &= 0, \\ w_0 &= \frac{du_0}{dr} / k_0. \end{aligned} \quad (2.12a, b, c)$$

The equations (2.12a,b) are consistent if

$$\begin{aligned} k_0^2 &= (3-f)i \\ \text{or } k_0^2 &= -(1+f)i \end{aligned} \quad (2.13a, b)$$

which correspond to the  $j = 3$  and  $j = 2$  modes respectively. At higher order  $u_0$ , and hence  $v_0, w_0$  and  $p_0$ , are determined as solvability conditions. We find that (2.13a,b) respectively lead to

$$u_0 = J_2(s_n r), \quad u_0 = J_0(t_n r) \quad (2.14a, b)$$

where

$$J_2(s_n) = J_0(t_n) = 0.$$

A more detailed derivation of (2.14) is found in HSG. Thus (2.13a,b) correspond to two countably infinite sets of eigenvalues and  $\{s_n\}, \{t_n\}$  determine the order  $Re^{-\frac{1}{2}}$  correction terms in the expansion of  $k$ . In fact the appropriate equations are found to be

$$k_1 = \frac{-(1-i)(4-f)s_n^2}{2\sqrt{2(3-f)^3}} \quad (2.15)$$

and

$$k_1 = \frac{-(2+f)t_n^2(1+i)}{2\sqrt{2}(1+f)^{3/2}}. \quad (2.16)$$

Henceforth we refer to the eigenvalues corresponding to (2.13a,b) using the indices  $j = 3$  and  $j = 2$  respectively. The structure outlined above breaks down when  $n$  is formally  $O(Re)$  in which case the eigenfunction has both axial and radial variations on the  $Re^{-\frac{1}{2}}$  lengthscale. We can now modify the spatial eigenvalue expansions (1.13a,b,c,d) using the asymptotic structure developed above; we therefore write:

$$\begin{aligned} u &= \sum_1^\infty \left[ \frac{\epsilon_n i}{\{3-f\}\{1+f\}} \left\{ \frac{(f+1)J_1(\mu_{1n}^0 r)}{r} + (1-f)\mu_{1n}^0 J_0(\mu_{1n}^0 r) \right\} \frac{\sin k_{1n}^0 x}{\sin k_{1n}^0 A} \right. \\ &\quad \left. + \gamma_n J_0(t_n r) \frac{\sin \lambda_2 x}{\sin \lambda_2 A} + \beta_n J_2(s_n r) \frac{\sin \lambda_1 x}{\sin \lambda_1 A} \right] + \dots, \\ v &= \sum_1^\infty \left[ \frac{\epsilon_n}{\{3-f\}\{1+f\}} \left\{ -(1+f) \frac{J_1(\mu_{1n}^0 r)}{r} + 2\mu_{1n}^0 J_0(\mu_{1n}^0 r) \right\} \frac{\sin k_{1n}^0 x}{\sin k_{1n}^0 A} \right. \\ &\quad \left. - i\gamma_n J_0(t_n r) \frac{\sin \lambda_2 x}{\sin \lambda_2 A} + i\beta_n J_2(s_n r) \frac{\sin \lambda_1 x}{\sin \lambda_1 A} \right] + \dots, \\ w &= \sum_1^\infty \frac{\epsilon_n i k_{1n}^0}{(f-1)} J_1(\mu_{1n}^0 r) \frac{\cos k_{1n}^0 x}{\sin k_{1n}^0 A} + \dots, \\ p &= \sum_1^\infty \epsilon_n J_1(\mu_{1n}^0 r) \frac{\sin k_{1n}^0 x}{\sin k_{1n}^0 A} + \dots. \end{aligned} \quad (2.17a, b, c, d)$$

where

$$\lambda_1 = (1 + i)\sqrt{\frac{3-f}{2}}\sqrt{Re}, \quad \lambda_2 = (1 - i)\sqrt{\frac{1+f}{2}}\sqrt{Re}.$$

We now apply the endwall condition (1.12c) on the axial velocity component  $w$  to give

$$-2if r = \sum_1^{\infty} \frac{\epsilon_n i k_{1n}^0}{(f-1)} J_1(\mu_{1n}^0 r) \cot k_{1n}^0 A$$

so that after multiplying both sides of the equation by  $r J_1(\mu_{1n}^0 r)$ , integrating from  $r = 0$  to  $r = 1$  and using the well-known properties of Bessel functions we obtain

$$\epsilon_n = \frac{4f(3-f) \tan k_{1n}^0 A}{k_{1n}^0 (\mu_{1n}^0)^2 \left\{ 1 + \frac{1}{(k_{1n}^0)^2} \right\} J_1(\mu_{1n}^0)} \quad (2.18)$$

while the endwall conditions on the radial and circumferential velocity components yield equations which can be solved for  $\{\beta_n\}$  and  $\{\gamma_n\}$  in terms of  $\{\epsilon_n\}$ . It is at this stage that the differences between the finite and infinite Reynolds number have emerged. Thus the amplitude functions  $\{\epsilon_n\}$ ,  $\{\beta_n\}$  and  $\{\gamma_n\}$  in the limit  $Re$  approaches  $\infty$  can be found explicitly using orthogonality properties of Bessel functions. At finite values of  $Re$  HSG found it necessary to use either collocation or a least squares approach in order to find the corresponding amplitudes. At higher order in the procedure that we have begun above, the sidewall boundary layer comes into play at the endwalls; at that stage the higher order amplitude coefficients must be found by collocation or the least squares method.

It follows from (2.17d) and (2.18) that  $p$  on the endwall,  $x = A$ , can be expressed as the infinite series

$$p = 4f(3-f) \sum_1^{\infty} \frac{k_{1n}^0 \tan k_{1n}^0 A J_1(\mu_{1n}^0 r)}{(\mu_{1n}^0)^2 J_1(\mu_{1n}^0) [1 + (k_{1n}^0)^2]}, \quad (2.19)$$

which is correct up to order  $Re^0$ .

### The pressure coefficient

We shall now use the high Reynolds number form of the spatial eigenvalue approach to find the pressure exerted by the fluid on the container. Since almost all of the available experimental results for pressure correspond to measurements made at the endwall we shall concentrate on that situation. More precisely we use our theory to find the amplitude of the pressure measured by a pressure transducer located at the endwall. More detail of the derivation of this pressure coefficient can be found in Gerber et al.<sup>[4]</sup>

First we note that  $p^+$ , the pressure calculated from the Navier-Stokes equations is

$$p^+ = \frac{1}{2} r^2 - K_0 p^*,$$

in the case  $K_0 \rightarrow 0$ . We must now relate our calculations in an inertial frame to the frame  $\tilde{r}, \tilde{\theta}, \tilde{x}$  used in HSG where the  $\tilde{x}$  axis coincides with the cylinder axis. A routine calculation based on a Taylor series expansion shows that, for example

$$\frac{1}{2}r^2 = \frac{1}{2}\tilde{r}^2 - K_0\tilde{r}\tilde{x}\cos\{ft - \tilde{\theta}\} + O(K_0^2).$$

We now let  $\Delta p$  be the disturbance pressure not including the contribution from solid body rotation. At points fixed on the surface of the cylinder

$$\Delta p = \frac{1}{2}r^2 - K_0 p^*(\tilde{r}, \tilde{\theta}, \tilde{x}, t) - \frac{1}{2}\tilde{r}^2$$

and since  $p^*(\tilde{r}, \tilde{\theta}, \tilde{x}, t) - p^*(r, \theta, x, t) = O(K_0)$  it follows that

$$\Delta p = -K_0[-\underline{p}_i \sin(ft - \theta) + (\underline{p}_r + rx) \cos(ft - \theta)] + O(K_0^2).$$

Here subscripts  $r$  and  $i$  denote the real and imaginary parts of a complex quantity. Now since

$$\underline{p}_r + rx = p_r + f^2 rx, \quad \underline{p}_i = p_i$$

the pressure coefficient  $c_p = \frac{|\Delta p|}{K_0}$  may be written as

$$c_p = \sqrt{(\underline{p}_r + rx)^2 + p_i^2}. \quad (2.20)$$

It then follows from (2.19) and (2.20) that  $c_p$  calculated using the spatial eigenvalue approach in the limit  $Re \rightarrow \infty$  is given by

$$c_p = \left| \frac{4f(1-f)^2}{1+f} \sum_1^\infty \frac{\tan k_{1n}^0 A J_1(\mu_{1n}^0 r)}{k_{1n}^0 [1 + (k_{1n}^0)^2] J_1(\mu_{1n}^0)} + f^2 r A \right| + O(Re^{-\frac{1}{2}}). \quad (2.21)$$

The above equation is not uniformly valid since at the Stewartson eigenfrequencies the unperturbed state can support neutral eigenfunctions. However, it is clear that  $c_p$  will become unbounded if  $k_{1n}^0$  corresponds to one of the Stewartson eigenvalues in which case  $\tan k_{1n}^0 A = \infty$ . In fact our expansion procedure is readily modified to take account of this possibility. Suppose then that  $f$  is an eigenfrequency  $\bar{f}$  of the inviscid problem. Without any loss of generality we can suppose that  $k_{11}^0 A = \pi/2$  so that  $\epsilon_1$  is formally infinite. In order to remove this singularity we note from (2.18) that if higher order terms are retained then  $\epsilon_1$  is in fact  $O(Re^{\frac{1}{2}})$  when  $f = \bar{f}$ . Since  $k_{1n}^0 = k_{1n}^0(f)$  and we wish to obtain a correct zeroth order approximation to  $c_p$  for all values of  $f$  we must therefore

modify (2.17) for  $f - \bar{f} \sim 0(Re^{-\frac{1}{2}})$ . Thus (2.21) is the correct zeroth order approximation to  $c_p$  for  $f - \bar{f} \gg 0(Re^{-\frac{1}{2}})$ ; we refer to this situation as the nonresonant case.

It follows from our calculations above for the nonresonant case by taking the limit  $f \rightarrow \bar{f}$  that  $\epsilon_1, \{\beta_n\}, \{\gamma_n\}$  for all  $n$  becomes formally  $0(Re^{+\frac{1}{2}})$  when  $f - \bar{f} = 0(Re^{-\frac{1}{2}})$ .

We therefore make use of the new scalings inferred above and therefore replace (2.17) by

$$\begin{aligned}
u &= \frac{i\epsilon_1\sqrt{Re}}{(3-f)(1+f)} \left\{ \frac{(1+f)}{r} J_1(\mu_{11}^0 r) + (1-f)\mu_{11}^0 J_0(\mu_{11}^0 r) + \dots \right\} \frac{\sin k_{11}x}{\sin k_{11}A} \\
&+ \sum_2^\infty \frac{\epsilon_n i}{(3-f)(1+f)} \left\{ \frac{1+f}{r} J_1(\mu_{1n}^0 r) + (1-f)\mu_{1n}^0 J_0(\mu_{1n}^0 r) + \dots \right\} \frac{\sin k_{1n}^0 x}{\sin k_{1n}^0 A} \\
&+ \sqrt{Re} \sum_1^\infty \gamma_n J_0(t_n r) \frac{\sin \lambda_2 x}{\sin \lambda_2 A} + \dots \\
&+ \sqrt{Re} \sum_1^\infty \beta_n J_2(s_n r) \frac{\sin \lambda_1 x}{\sin \lambda_1 A} + \dots \\
v &= \frac{\epsilon_1\sqrt{Re}}{(3-f)(1+f)} \left\{ -(1+f) \frac{J_1(\mu_{11}^0 r)}{r} + 2\mu_{11}^0 J_0(\mu_{11}^0 r) + \dots \right\} \frac{\sin k_{11}x}{\sin k_{11}A} \\
&+ \sum_2^\infty \frac{\epsilon_n}{(3-f)(1+f)} \left\{ \frac{-(f+1)J_1(\mu_{1n}^0 r)}{r} + 2\mu_{1n}^0 J_0(\mu_{1n}^0 r) + \dots \right\} \frac{\sin k_{1n}^0 x}{\sin k_{1n}^0 A} \\
&+ \sqrt{Re} \sum_1^\infty i\beta_n J_2(s_n r) \frac{\sin \lambda_1 x}{\sin \lambda_1 A} + \dots \\
&- \sqrt{Re} \sum_1^\infty i\gamma_n J_0(t_n r) \frac{\sin \lambda_2 x}{\sin \lambda_2 A} + \dots \\
w &= \frac{ik_{11}^0}{(f-1)} \epsilon_1 \sqrt{Re} [J_1(\mu_{11}^0 r) + \dots] \frac{\cos k_{11}x}{\sin k_{11}A} \\
&+ \sum_2^\infty \frac{ik_{1n}^0}{(f-1)} \epsilon_n [J_1(\mu_{1n}^0 r) + \dots] \frac{\cos k_{1n}^0 x}{\sin k_{1n}^0 A} \\
&+ \sum_1^\infty \frac{s_n \beta_n J_2'(s_n r)(1-i)}{\sqrt{3-f}\sqrt{2}} \frac{\cos \lambda_1 x}{\sin \lambda_1 A} + \dots \\
&+ \sum_1^\infty \frac{-\gamma_n t_n J_1(t_n r)(1+i)}{\sqrt{1+f}\sqrt{2}} \frac{\cos \lambda_2 x}{\sin \lambda_2 A} + \dots \\
p &= \epsilon_1 \sqrt{Re} J_1(\mu_{11}^0 r) \frac{\sin k_{11}x}{\sin k_{11}A} + 0(1),
\end{aligned}$$

(2.22a, b, c, d)

We note that in the above expansion  $f$  formally differs from  $\bar{f}$  by  $O(Re^{-\frac{1}{2}})$ . If we now apply the endwall conditions on the radial and circumferential velocity components we find, after using the well-known orthogonality properties of Bessel functions, that

$$\begin{aligned}\gamma_n J_1^2(t_n) &= \frac{-\mu_{11}^0 \epsilon_1 i}{(1+f)} \int_0^1 r J_0(\mu_{11}^0 r) J_0(t_n r) dr, \\ \beta_n [J_2'(s_n)]^2 &= \frac{-i \epsilon_1 \mu_{11}^0}{(3-f)} \int_0^1 r J_2(\mu_{11}^0 r) J_2(s_n r) dr.\end{aligned}\quad (2.23a, b).$$

The endwall condition (1.12c) on the axial velocity component then gives

$$\begin{aligned}\frac{ik_{11} \epsilon_1 \sqrt{Re}}{(f-1)} J_1(\mu_{11}^0 r) \cot k_{11} A + \sum_2^\infty \frac{\epsilon_n i k_{1n}^0}{(f-1)} J_1(\mu_{1n}^0 r) \cot k_{1n}^0 A \\ + \sum_1^\infty \frac{s_n \beta_n J_2'(s_n r) (1-i) \cot \lambda_1 A}{\sqrt{2} \sqrt{3-f}} \\ + \sum_1^\infty \frac{-\gamma_n t_n J_1(t_n r) (1+i) \cot \lambda_2 A}{\sqrt{2} \sqrt{1+f}} = -2if r.\end{aligned}$$

We now multiply the above equation by  $r J_1(\mu_{11}^0 r)$  and integrate from  $r = 0$  to  $r = 1$  and replace  $\beta_n$  and  $\gamma_n$  using (2.23). After some manipulations we can show that

$$\begin{aligned}\epsilon_1 \left[ \frac{\sqrt{Re}}{2} \cot k_{11} A \left( 1 + \frac{1}{(k_{11})^2} \right) J_0^2(\mu_{11}^0) \left( \frac{f-1}{f+1} \right)^2 \frac{(\mu_{11}^0)^2 i k_{11}}{f-1} \right. \\ \left. - \frac{(1+i) \cot \lambda_1 A}{\sqrt{2} (3-f)^{3/2}} (\mu_{11}^0) J_0(\mu_{11}^0) S_1 \right. \\ \left. - \frac{(1-i) \cot \lambda_2 A}{\sqrt{2} (1+f)^{3/2}} (\mu_{11}^0)^2 J_0^2(\mu_{11}^0) S_2 \right] \\ = \frac{-2if}{\mu_{11}^0} J_2(\mu_{11}^0)\end{aligned}\quad (2.24)$$

where

$$\begin{aligned}S_1 &= \sum_1^\infty \frac{s_n z_n}{[(\mu_{11}^0)^2 - s_n^2] J_1(s_n)} \\ S_2 &= \sum_1^\infty \frac{t_n^2}{[(\mu_{11}^0)^2 - t_n^2]^2}\end{aligned}$$

Here  $z_n = \int_0^1 r J_2'(s_n r) J_1(\mu_{11}^0 r) dr$ . We note that in (2.24)  $\sqrt{Re} \cot k_{11} A \sim O(Re^0)$  because  $f$  differs from  $\bar{f}$  by  $O(Re^{-\frac{1}{2}})$ . Finally we note that  $\cot \lambda_1 A$  and  $\cot \lambda_2 A$  to this order can be

replaced by  $-i$  and  $+i$  respectively. Thus with  $\epsilon_1$  given by (2.24) the pressure perturbation is

$$p = \epsilon_1 \sqrt{Re} J_1(\mu_{11}^0 r) \quad (2.25)$$

which is of course  $O(Re^{\frac{1}{2}})$  larger than that in the non-resonant case. It can be shown from (2.24) that when  $1 \gg f - \bar{f} \gg Re^{-\frac{1}{2}}$  the equation (2.25) is consistent with that obtained from (2.19) by taking the limit  $f \rightarrow \bar{f}$ . Thus the formula

$$p = \epsilon_1 \sqrt{Re} J_1(\mu_{11}^0 r) + \sum_2^{\infty} \frac{4f(1-f)^2}{(1+f)} \frac{\tan k_{1n} A J_1(\mu_{1n}^0 r)}{(k_{1n}^0)[1 + (k_{1n}^0)^2] J_1(\mu_{1n}^0)} \quad (2.26)$$

gives a correct zeroth order approximation to  $p$  for all  $f$ . The pressure coefficient  $c_p$  is thus given by

$$c_p = \left| \frac{4f(1-f)^2}{1+f} \sum_2^{\infty} \frac{\tan k_{1n}^0 A J_1(\mu_{1n}^0 r)}{(k_{1n}^0)[1 + (k_{1n}^0)^2] J_1(\mu_{1n}^0)} + f^2 r A + \epsilon_1 \sqrt{Re} J_1(\mu_{11}^0 r) \right| \quad (2.27)$$

with  $\epsilon_1$  given by (2.24).

We close this section with a discussion of the relationship between our resonant expansion procedure discussed above with the viscous correction to Stewartson's inviscid theory given by Wedemeyer<sup>[6]</sup>. In the latter paper Wedemeyer showed how a viscous correction to the inviscid theory could be obtained by considering viscous boundary layers at the ends and sidewall of the cylinder. (We observe that  $\alpha$  and  $\beta$  of Eqs.(33a) and (33b) of Reference 6 are related to  $\lambda_1$  and  $\lambda_2$  on p.9 of this paper as follows:  $\lambda_1 = i\alpha\alpha$ ,  $\lambda_2 = -i\alpha\beta$ .) We note that away from the endwalls the terms that appear inside the summation signs in (2.22) are exponentially small. The term that remains in the expressions for the velocity and pressure corresponds to Stewartson's eigenvalue. However the axial wavenumber used there is  $k_{11}$  correct to order  $Re^{-1/2}$ . Thus there is a viscous correction in our expansion that arises from the fact that we choose to continue the inviscid expansion in order to take care of the viscous sidewall layer. Thus the modified eigenfunction we have used is precisely that implied by Wedemeyer's equation (16). At the ends of the cylinder all the ratios of the trigonometric functions are  $O(1)$  so that all the terms are to be retained. Now the terms proportional to  $\sin(\lambda_j x)$ ,  $\cos(\lambda_j x)$  are needed in order to satisfy the endwall conditions. If we choose to look at the unforced problem, then it can be shown that the effect of these terms is exactly equivalent, in a formal asymptotic sense, to Wedemeyer's conditions (18,19). Thus, for the unforced problem at the resonant frequency, our expansion is equivalent to that of Wedemeyer. Notice, however, that the form of our expansion

enables us to determine in a precise asymptotic form the forced velocity field both at the resonant frequency and elsewhere. That is not the case for Wedemeyer's theory so we can interpret (2.22) as being a generalization of Wedemeyer's work to the forced problem at all frequencies.

### 3. Results and Discussion

We shall give results only for the composite expansion (2.27) rather than plotting separately the resonant and non-resonant expansions. In particular we will compare our results with those of Whiting<sup>[7]</sup> who investigated the problem experimentally. In Figures 3a,b,c we compare with experimental data for the pressure coefficient measured at  $r = .668$  with  $A = 3.1481$  at three different values of the Reynolds number. Also shown in these figures are curves representing theoretical results from Gerber et al.<sup>[4]</sup> and Murphy<sup>[8]</sup>. Both of the latter calculations used approximate endwall conditions obtained using Wedemeyer's approach. At  $Re = 5 \times 10^3$  the results of the present approach and Reference 7 agree more closely with experiment than the results of Reference 4 theory. At  $Re = 10^5$  the present theory gives as good agreement with the theory as the other approaches but at the highest value of the Reynolds number our method overestimates the pressure coefficient at the resonant frequency. Apart from the immediate neighborhood of the resonant frequency the different theoretical approaches at the two highest values of  $Re$  are in agreement. The difference between the predicted resonant response and the experimental data could presumably be eliminated by proceeding with the present calculation to the next order.

In Figure 4 we show a similar comparison at  $A = 1.0509$ ; again we see that the differences in the two approaches are small except for a small interval near the resonant frequency. In Figure 5 we show the variation of the resonant frequency with Reynolds number for  $A = 3.1481$ .

In Figure 6 we show 3D plots of the pressure coefficient at two different Reynolds numbers over a portion of the aspect ratio-frequency plane. Equal intervals in  $f$  and  $A$  are used in these plots. The localized peaks correspond to resonant responses caused by the excitation of one of the Stewartson modes. Such plots are useful in picking out portions of parameter space with certain properties; more detailed plots or variations can be obtained from the program written to calculate  $c_p$ . A few points about the approach that we have developed here are in order:

1. The composite expansion is relevant whenever any one of the Stewartson eigenvalues occurs; the eigenvalue whose eigenfunction is rescaled by a factor  $\sqrt{Re}$  is taken to be that eigenvalue.

2. The computational time for the present approach is comparable to that required for the different approaches mentioned above. For example all the calculations used to supply the data for the 3D plots (with 2500 nodes) were carried out in about one hour on an Olivetti M24 PC.

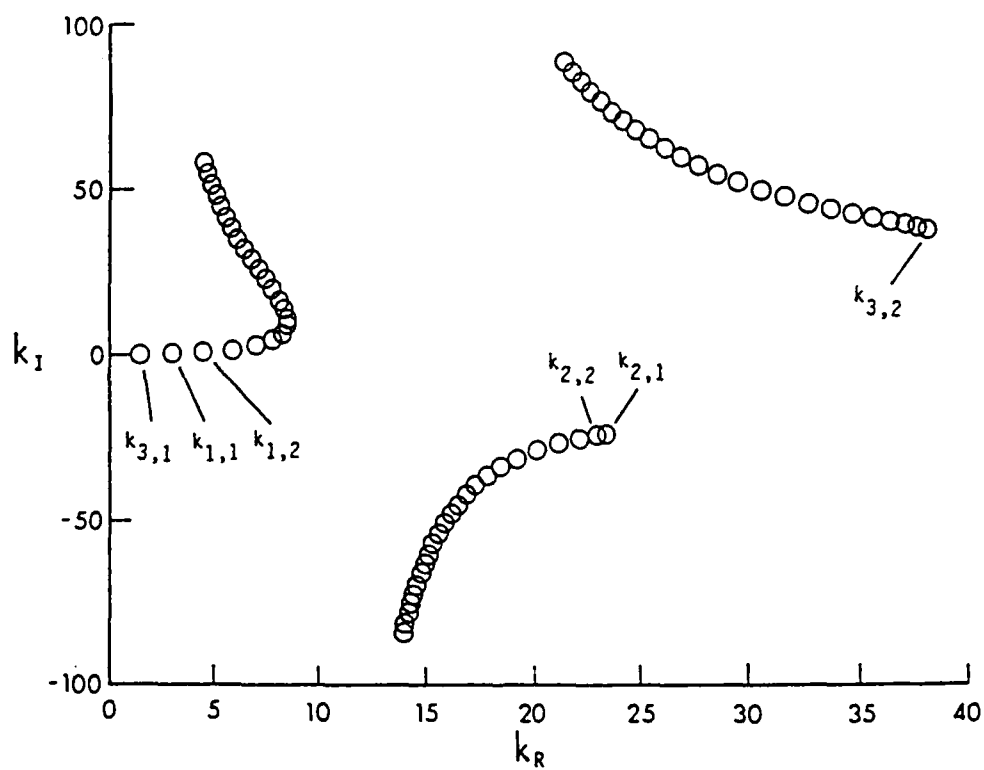


Figure 1. The first 72 eigenvalues for  $Re = 1000, f = 0.1$   
(taken from Reference 2).

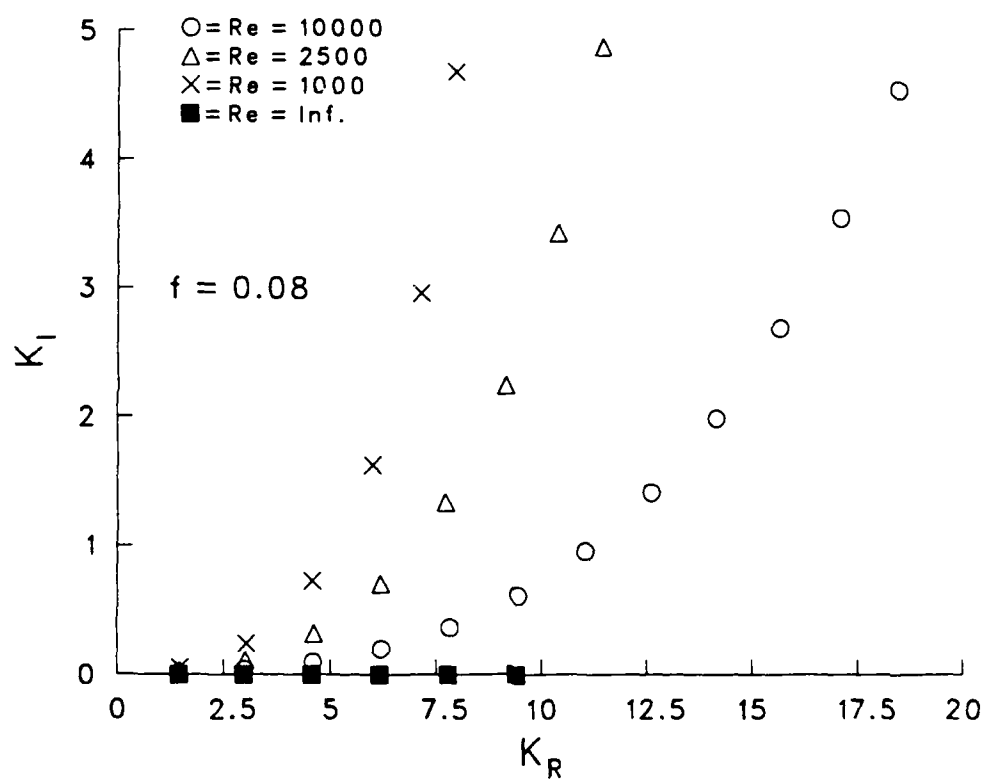


Figure 2. The eigenvalue spectrum for some large values of  $Re$  and  $f = 0.08$

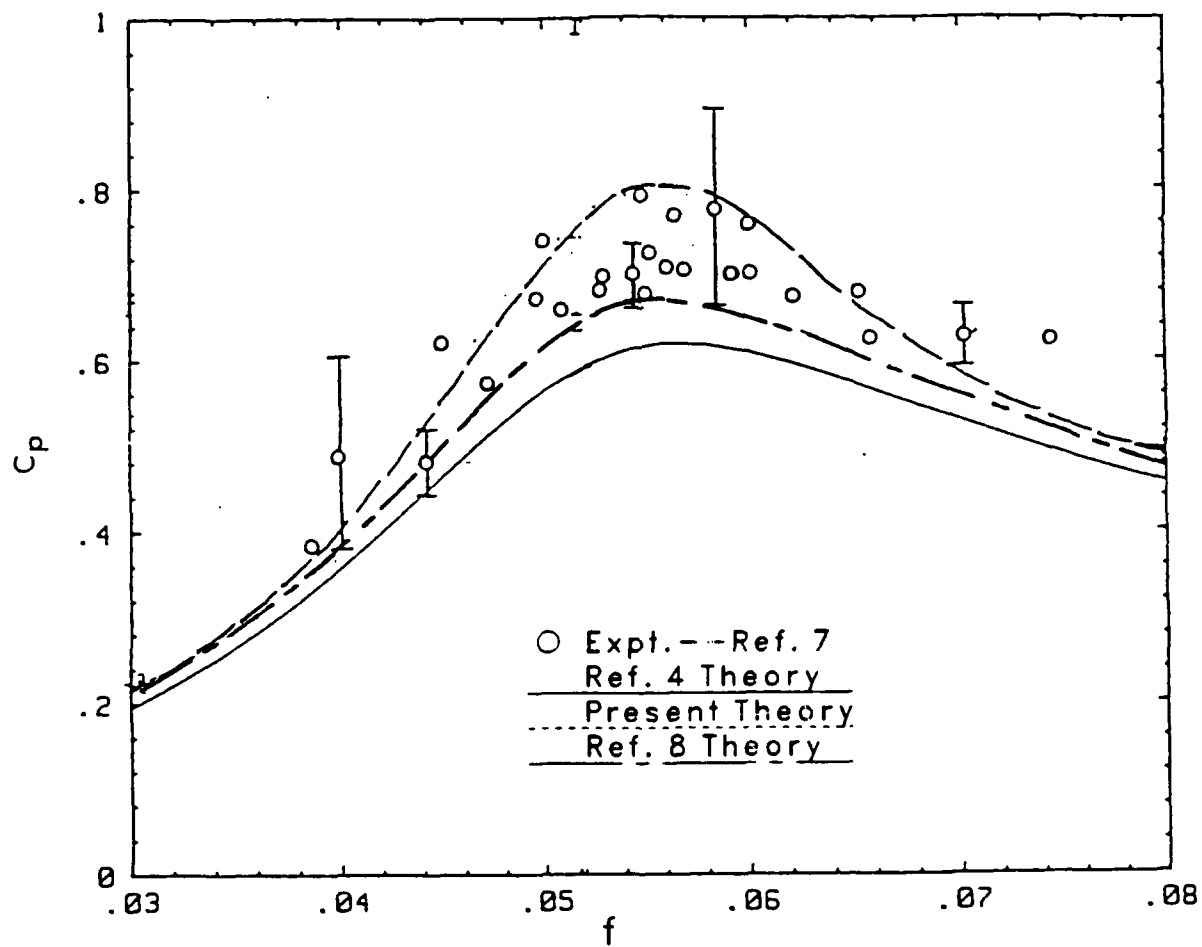


Figure 3a. The behavior of  $c_p$  calculated using the composite expansion with  $A = 3.1481$ ,  $Re = 5000$ . The experimental points are from Reference 7.

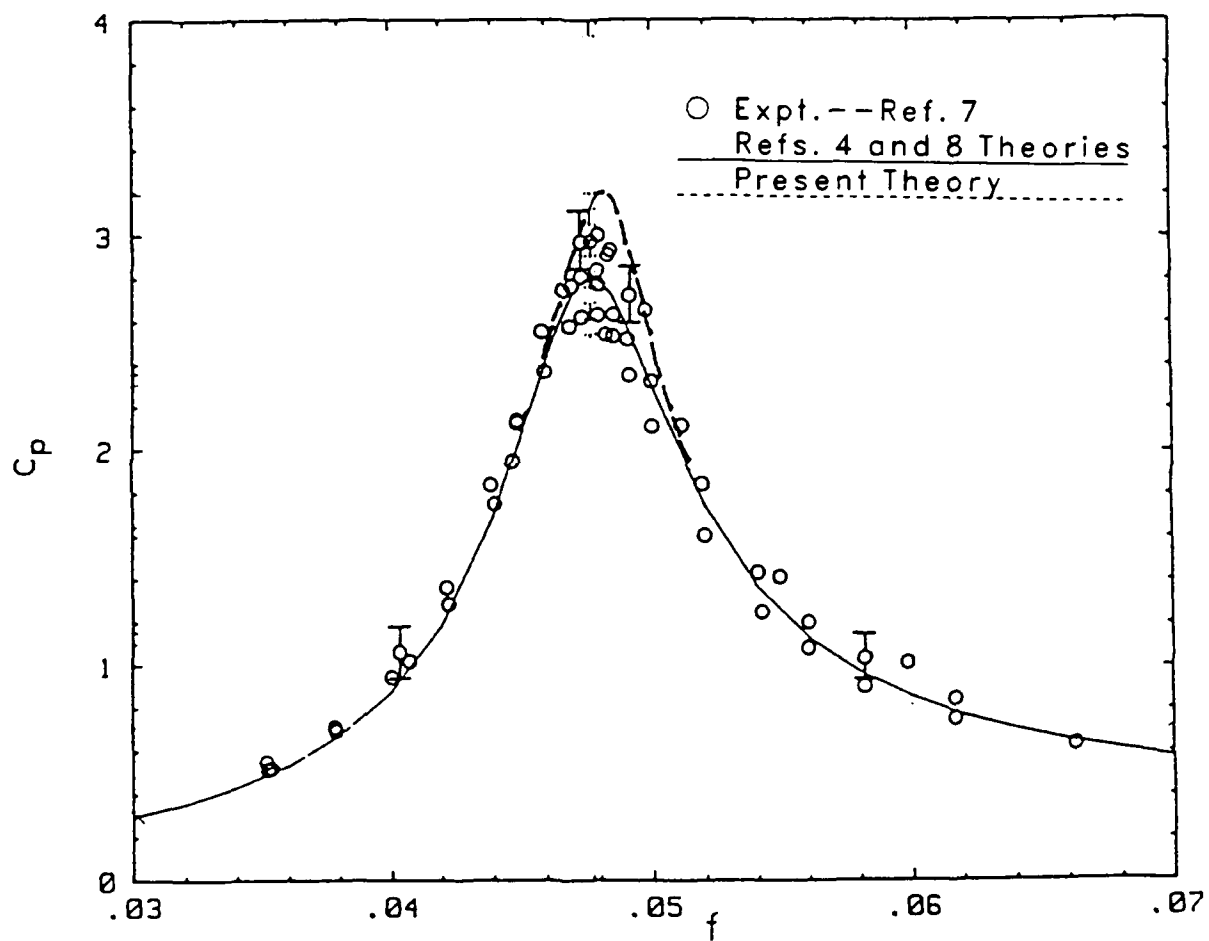


Figure 3b. The behavior of  $c_p$  calculated using the composite expansion with  $A = 3.1481$ ,  $Re = 100,000$ .

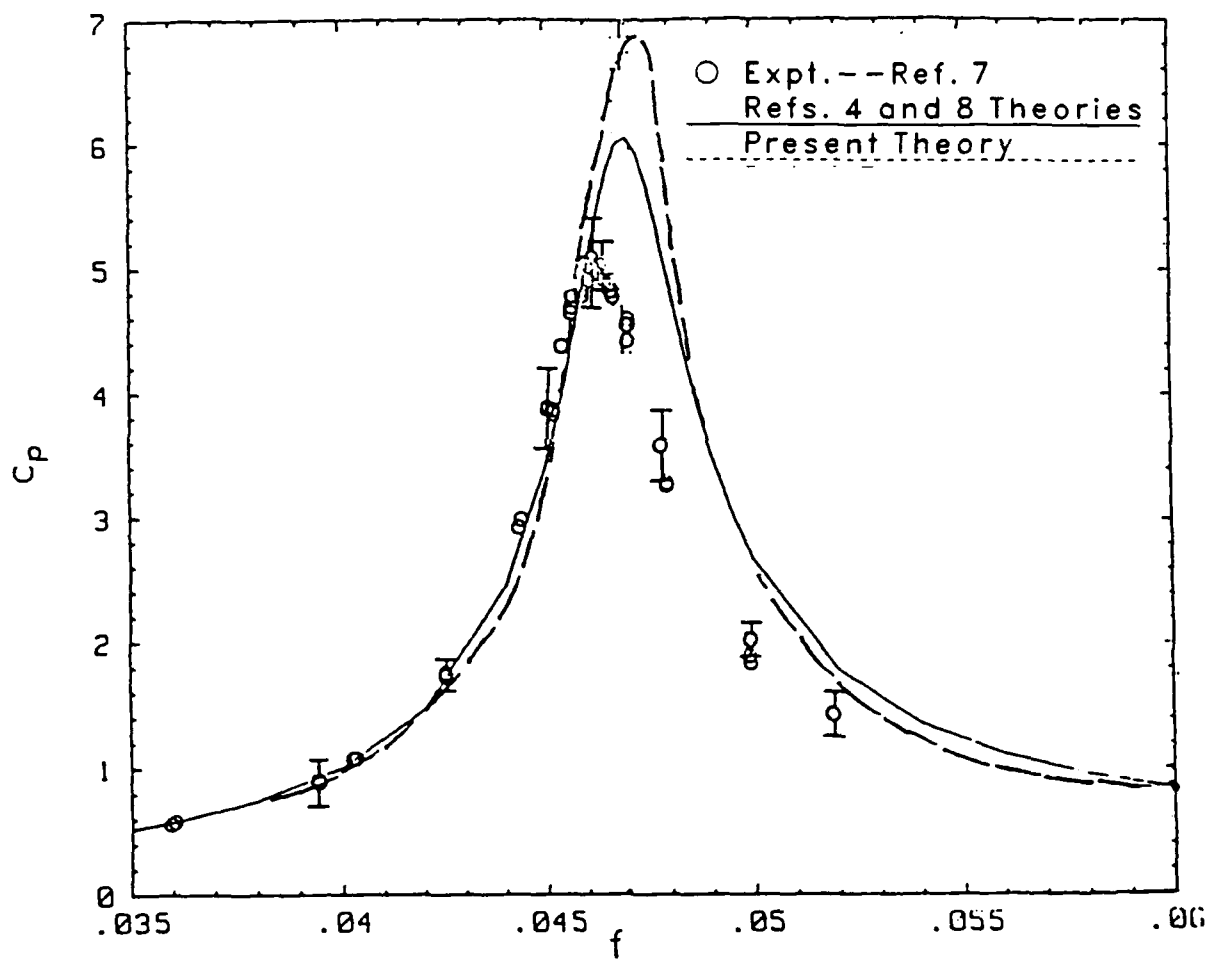


Figure 3c. The behavior of  $c_p$  calculated using the composite expansion with  $A = 3.1481$ ,  $Re = 500,000$ .

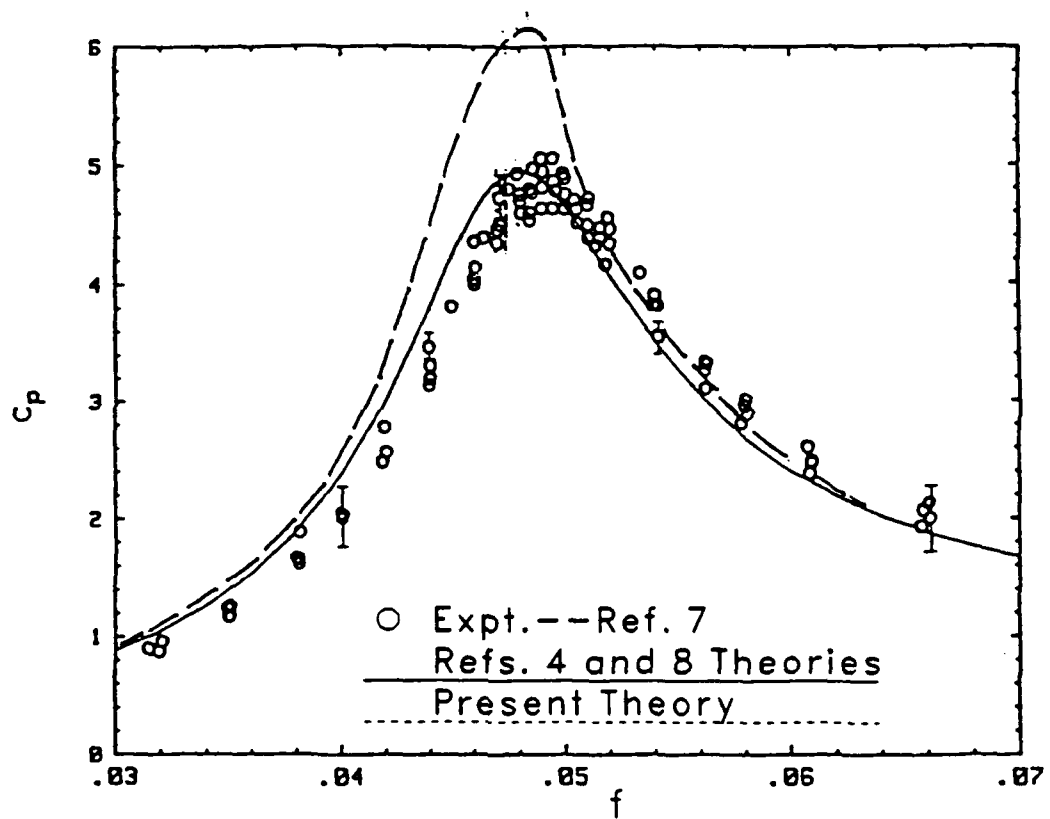


Figure 4a. The behavior of  $c_p$  calculated using the composite expansion with  $A = 1.0509$ ,  $Re = 100,000$ .

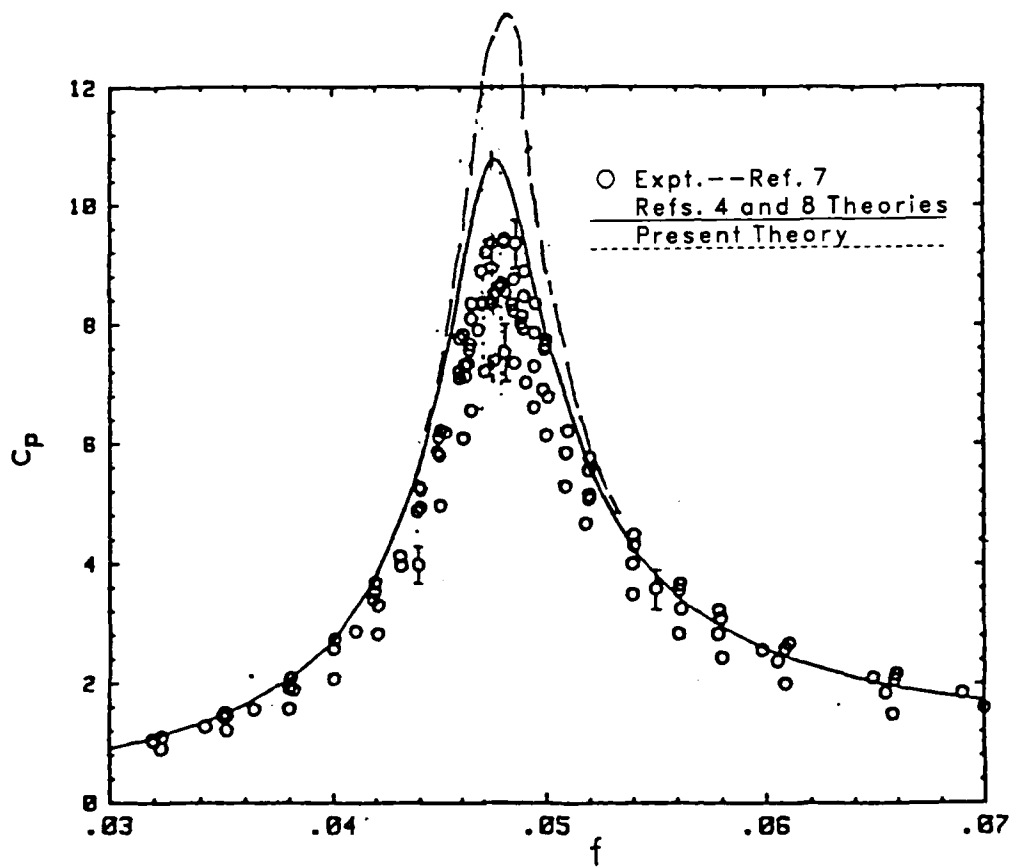


Figure 4b. The behavior of  $c_p$  calculated using the composite expansion with  $A = 1.0509$ ,  $Re = 500,000$ .

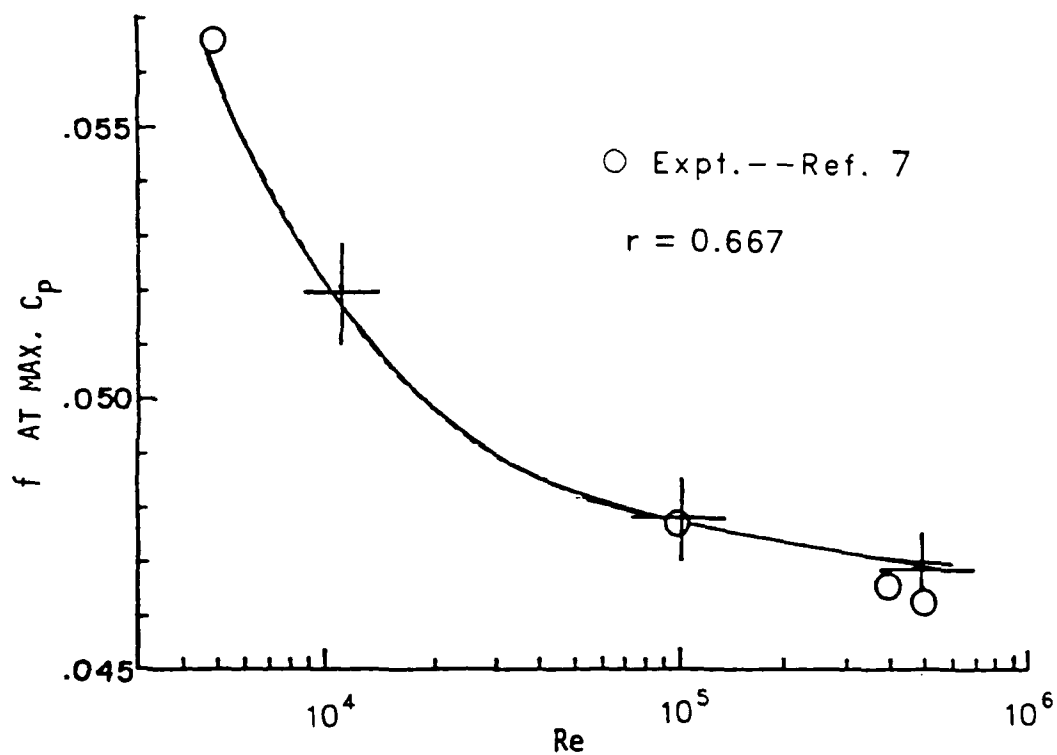


Figure 5. Variation of the frequency of peak response with Re for  $A = 3.148$ . Solid line is from the approach of Reference 4. The crosses are from the present calculations.

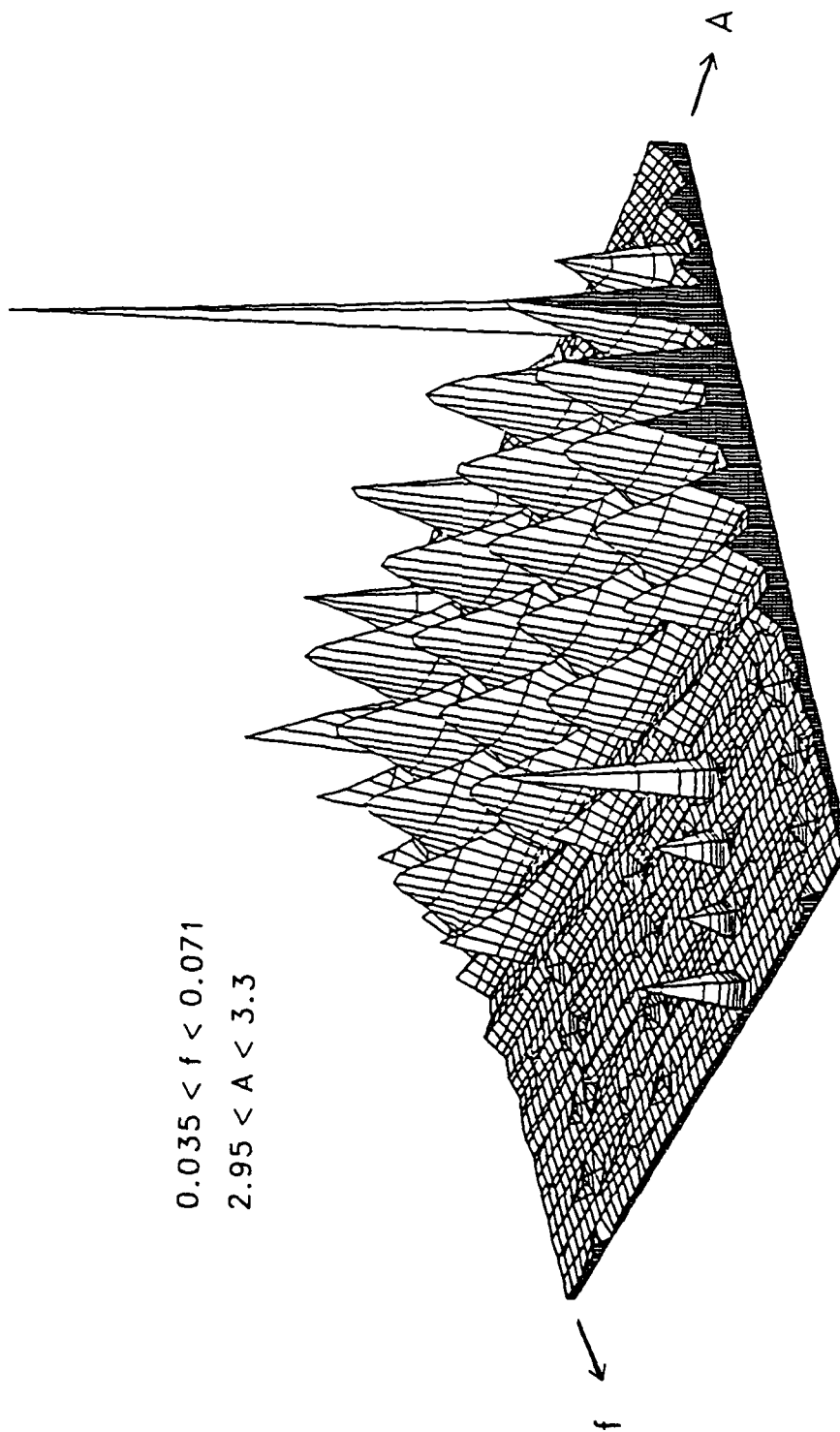


Figure 6a. A 3D plot of  $c_p$  against A and f for the case  $Re = 100,000$ .

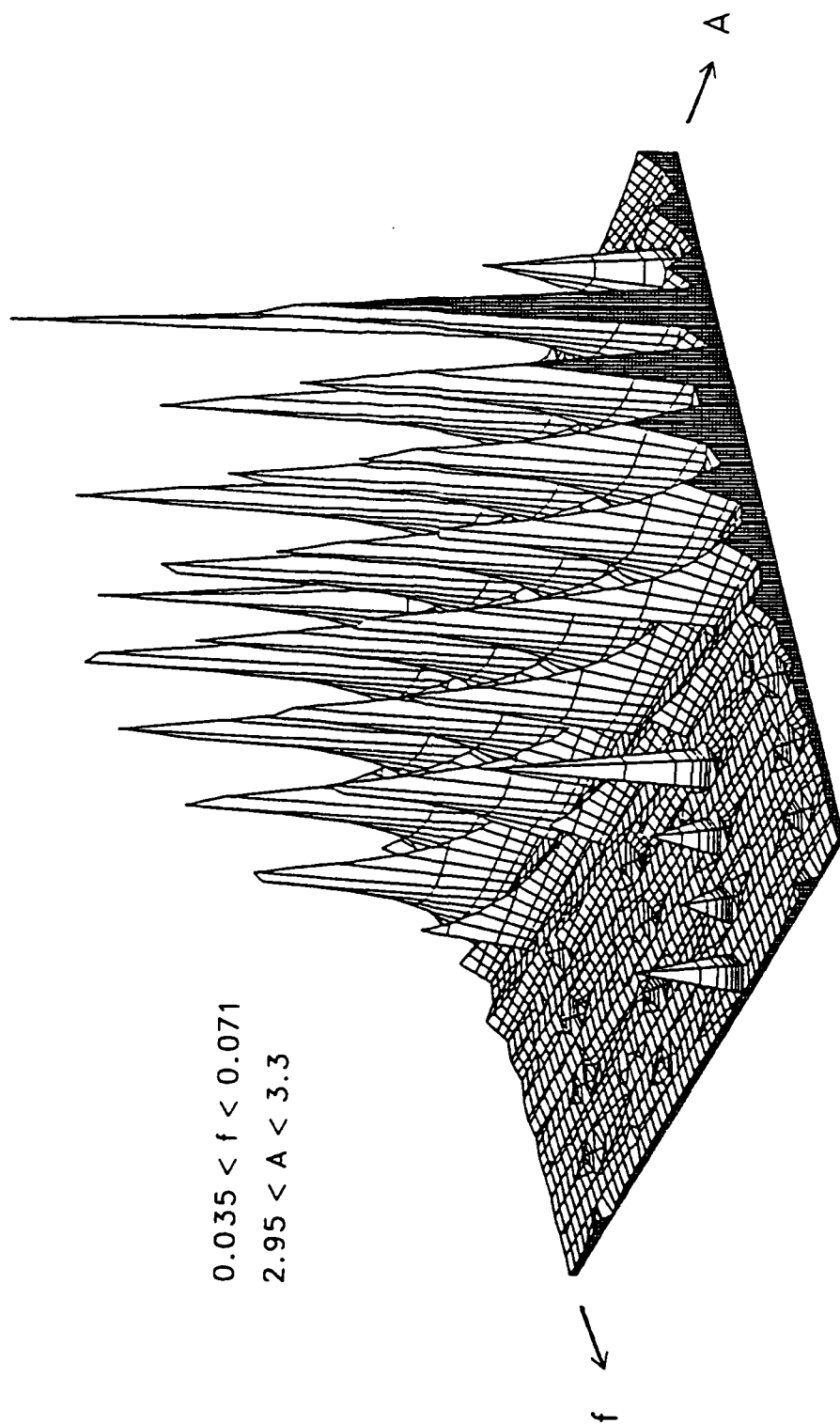


Figure 6b. A 3D plot of  $c_p$  against  $A$  and  $f$  for the case  $Re = 500,000$ .

INTENTIONALLY LEFT BLANK.

## REFERENCES

1. Vaughn, H.R., Oberkampf, W. and Wolfe, W.R., "Fluid Motion Inside a Spinning Nutating Cylinder", Journal of Fluid Mechanics, Vol. 150, pp. 121-138, 1985. Also "Numerical Solution for a Spinning, Nutating Fluid-Filled Cylinder", Sandia Report SAND 83-1789, December 1983.
2. Hall, P., Sedney, R. and Gerber, N., "Fluid Motion in a Spinning, Coning Cylinder via Spatial Eigenfunction Expansion", BRL-TR-2813, U.S. Army Ballistic Research Laboratory, Aberdeen Proving Ground, Maryland, August, 1984. (AD A190758) Also to appear in AIAA Journal.
3. Batchelor, G.K. and Gill, A.E., "Analysis of the Stability of Axisymmetric Jets", Journal of Fluid Mechanics, Vol. 14, pp. 529-551, 1962.
4. Gerber, N., Sedney R. and Bartos, J.M., "Pressure Moment on a Liquid-Filled Projectile: Solid Body Rotation", ARBRL-TR-02422, U.S. Army Ballistic Research Laboratory, Aberdeen Proving Ground, Maryland, October 1982. (AD A120567)
5. Stewartson, K., "On the Stability of a Spinning Top Containing Liquid", Journal of Fluid Mechanics, Vol. 5, Part 4, September 1959, pp. 577-592.
6. Wedemeyer, E.H., "Viscous Corrections to Stewartson's Stability Criterion," BRL Report No. 1325, Aberdeen Proving Ground, Maryland, June 1966. (AD 489687)
7. Whiting, R.D., "An Experimental Study of Forced Asymmetric Oscillations in a Rotating Liquid-Filled Cylinder", ARBRL-TR-02376, U.S. Army Ballistic Research Laboratory, Aberdeen Proving Ground, Maryland, October 1981. (AD A107948)
8. Murphy, C.H., "Angular Motion of a Spinning Projectile with a Viscous Liquid Payload", U.S. Army Ballistic Research Laboratory, Aberdeen Proving Ground, Maryland, ABRL-MR-03194, August 1982. (AD A118676) Also Journal of Guidance, Control, and Dynamics, Vol. 6, July-August 1983, pp. 280-286.

INTENTIONALLY LEFT BLANK.

No of Copies	Organization	No of Copies	Organization
1	Office of the Secretary of Defense OUSD(A) Director, Live Fire Testing ATTN: James F. O'Bryon Washington, DC 20301-3110	1	Director US Army Aviation Research and Technology Activity Ames Research Center Moffett Field, CA 94035-1099
(Unclass., unlimited) 12	Administrator	1	Commander US Army Missile Command ATTN: AMSMI-RD-CS-R (DOC) Redstone Arsenal, AL 35898-5010
(Unclass., limited) 2	Defense Technical Info Center		
(Classified) 2	ATTN: DTIC-DDA Cameron Station Alexandria, VA 22304-6145	1	Commander US Army Tank-Automotive Command ATTN: AMSTA-TSL (Technical Library) Warren, MI 48397-5000
1	HQDA (SARD-TR) WASH DC 20310-0001		
1	Commander US Army Materiel Command ATTN: AMCDRA-ST 5001 Eisenhower Avenue Alexandria, VA 22333-0001	1	Director US Army TRADOC Analysis Command ATTN: ATAA-SL White Sands Missile Range, NM 88002-5502
1	Commander US Army Laboratory Command ATTN: AMSLC-DL Adelphi, MD 20783-1145	(Class. only) 1	Commandant US Army Infantry School ATTN: ATSH-CD (Security Mgr.) Fort Benning, GA 31905-5660
2	Commander Armament RD&E Center US Army AMCCOM ATTN: SMCAR-MSI Picatinny Arsenal, NJ 07806-5000	(Unclass. only) 1	Commandant US Army Infantry School ATTN: ATSH-CD-CSO-OR Fort Benning, GA 31905-5660
2	Commander Armament RD&E Center US Army AMCCOM ATTN: SMCAR-TDC Picatinny Arsenal, NJ 07806-5000	1	Air Force Armament Laboratory ATTN: AFATL/DLODL Eglin AFB, FL 32542-5000
1	Director Benet Weapons Laboratory Armament RD&E Center US Army AMCCOM ATTN: SMCAR-CCB-TL Watervliet, NY 12189-4050		<u>Aberdeen Proving Ground</u>
1	Commander US Army Armament, Munitions and Chemical Command ATTN: SMCAR-ESP-L Rock Island, IL 61299-5000	2	Dir, USAMSAA ATTN: AMXSY-D AMXSY-MP, H. Cohen
1	Commander US Army Aviation Systems Command ATTN: AMSAV-DACL 4300 Goodfellow Blvd. St. Louis, MO 63120-1798	1	Cdr, USATECOM ATTN: AMSTE-TD
		3	Cdr, CRDEC, AMCCOM ATTN: SMCCR-RSP-A SMCCR-MU SMCCR-MSI
		1	Dir, VLAMO ATTN: AMSLC-VL-D

<u>No. of Copies</u>	<u>Organization</u>	<u>No. of Copies</u>	<u>Organization</u>
1	Commander Armament RD&E Center ATTN: SMCAR-AET-A (Mr. A. Loeb) Picatinny Arsenal, NJ 07806-5000	1	Director Office of Naval Research ATTN: Richard Whiting, Code 123 800 Quincy Street Arlington, VA 22217
1	Commander US Army Armament, Munitions and Chemical Command ATTN: AMSMC-IMP-L Rock Island, IL 61299-7300	2	AFWAL ATTN: J. S. Shang W. L. Hankey Wright-Patterson AFB, OH 45433
1	Commander, USACECOM R&D Technical Library ATTN: ASQNC-ELC-I-T, Myer Center Fort Monmouth, NJ 07703-5301	1	Aerospace Corporation Aero-Engineering Subdivision ATTN: Walter F. Reddall El Segundo, CA 90245
1	Director US Army Missile and Space Intelligence Center ATTN: AIAMS-YDL Redstone Arsenal, AL 35898-5500	5	Director National Aeronautics and Space Administration Ames Research Center ATTN: D. R. Chapman W. C. Rose B. Wick P. Kutler Tech Library Moffett Field, CA 94035
2	Director Sandia National Laboratories ATTN: Dr. W. Oberkampff Mr. W. O. Wolfe Albuquerque, NM 87185	4	Director National Aeronautics and Space Administration Langley Research Center ATTN: E. Price J. South J. R. Sterrett Tech Library Langley Station Hampton, BA 23365
2	Commander US Army Research Office ATTN: Dr. R. E. Singleton Dr. Jagdish Chandra P.O. Box 12211 Research Triangle Park, NC 27709-2211	1	Director National Aeronautics and Space Administration Lewis Research Center ATTN: MS 60-3, Tech Library 21000 Brookpark Road Cleveland, OH 44135-3127
2	Commander David W. Taylor Naval Ship Research and Development Command ATTN: H. J. Lugt, Code 1802 S. de los Santos Bethesda, MD 20084-5000	1	AVCO Systems Division ATTN: B. Reeves 201 Lowell Street Wilmington, MA 01887
1	Commander Naval Surface Warfare Center ATTN: DX-21 (Library Branch) Dahlgren, VA 22448		
3	Commander Naval Surface Warfare Center Applied Aerodynamics Division ATTN: M. Ciment A. E. Winklemann W. C. Ragsdale Silver Spring, MD 20910		

<u>No. of</u> <u>Copies</u>	<u>Organization</u>	<u>No. of</u> <u>Copies</u>	<u>Organization</u>
2	Director National Aeronautics and Space Administration Marshall Space Flight Center ATTN: Chief, S&E-AERO-AE (A.R. Felix) Dr. W.W. Fowles Huntsville, AL 35812	1	Hughes Aircraft ATTN: Dr. John McIntyre, Mail Code S41/B323 P.O. Box 92919 Los Angeles, CA 90009
1	Calspan Corporation ATTN: A. Ritter P.O. Box 400 Buffalo, NY 14225	1	Lockheed Missiles and Space Company ATTN: Tech Info Center 3251 Hanover Street Palo Alto, CA 94304
3	Aerospace Corporation ATTN: H. Mirels R.L. Varwig Aerophysics Lab P.O. Box 92957 Los Angeles, CA 90009	1	Martin-Marietta Corporation ATTN: H. Obremski 1450 S. Rolling Road Baltimore, Md 21227
2	Director Jet Propulsion Laboratory ATTN: L.M. Mach Tech Library 4800 Oak Grove Drive Pasadena, CA 91103	1	Arizona State University Department of Mechanical and Energy System Engineering ATTN: G.P. Neitzel Tempe, AZ 85281
3	Arnold Research Org., Inc. ATTN: J.D. Whitfield R.K. Matthews J.C. Adams Arnold AFB, TN 37389	1	Massachusetts Institute of Technology ATTN: H. Greenspan 77 Massachusetts Ave Cambridge, MA 02139
3	Boeing Commercial Airplane Company ATTN: R.A. Day, MS 1W-82 P.E. Rubbert, MS 3N-19 J.D. McLean, MS-3N-19 Seattle, WA 98124	2	North Carolina State University Mechanical and Aerospace Engineering Department ATTN: F.F. DeJarnette J.C. Williams Raleigh, NC 27607
2	Lockheed-Georgia Company ATTN: B.H. Little, Jr. G.A. Pounds, Dept 72074, Zone 403 86 South Cobb Drive Marietta, GA 30062	1	Notre Dame University Department of Aero Engineering ATTN: T.J. Mueller South Bend, IN 46556
1	General Dynamics ATTN: Research Library 2246 P.O. Box 748 Fort Worth, TX 76101	1	Northwestern University Department of Engineering Science and Applied Mathematics ATTN: Dr. S.H. Davis Evanston, IL 60201
2	Grumman Aerospace Corporation ATTN: R.E. Melnik L.G. Kaufman Bethpage, NY 11714	1	Ohio State University Department of Mechanical Engineering ATTN: Dr. T. Herbert Columbus, OH 43221
		2	Ohio State University Department of Aeronautical and Astronautical Engineering ATTN: S.L. Petrie O.R. Burggraf Columbus, OH 43210

<u>No. of Copies</u>	<u>Organization</u>
2	Polytechnic Institute of New York ATTN: G. Moretti Tech Library Route 110 Farmingdale, NY 11735
3	Princeton University James Forrestal Research Center Gas Dynamics Laboratory ATTN: S.M. Bogdonoff S.I. Cheng Tech Library Princeton, NJ 08540
1	Purdue University Thermal Science & Prop Center ATTN: Tech Library W. Lafayette, IN 47906
1	Rensselaer Polytechnic Institute Department of Math Sciences ATTN: Tech Library Troy, NY 12181
1	Rutgers University Department of Mechanical, Industrial, and Aerospace Engineering ATTN: R.H. Page New Brunswick, NJ 08903
1	Southern Methodist University Department of Civil and Mechanical Engineering ATTN: R.L. Simpson Dallas, TX 75272
1	Southwest Research Institute Applied Mechanics Reviews 8500 Culebra Road San Antonio, TX 78228
1	San Diego State University Department of Aerospace Engineering and Engineering Mechanics College of Engineering ATTN: K.C. Wang San Diego, CA 92115
1	Harvard University Division of Engineering and Applied Physics ATTN: G.J. Carrier Cambridge, MA 01238
1	Stanford University Department of Aeronautics/Astronautics ATTN: M. Van Dyke Stanford, CA 94305

<u>No. of Copies</u>	<u>Organization</u>
1	Texas A&M University College of Engineering ATTN: R.H. Page College Station, TX 77843
1	University of California - Davis ATTN: Dr. Harry A. Dwyer Davis, CA 95616
1	University of California - Berkeley Department of Aerospace Engineering ATTN: M. Holt Berkeley, CA 94720
1	University of California - San Diego Department of Aerospace Engineering and Mechanical Engineering Sciences La Jolla, CA 92037
1	University of Colorado Department of Astro-Geophysics ATTN: E.R. Benton Boulder, CO 80302
2	University of Maryland ATTN: W. Melnik J.D. Anderson College Park, MD 20740
1	University of Maryland - Baltimore County Department of Mathematics ATTN: Dr. Y.M. Lynn 5401 Wilkens Avenue Baltimore, MD 21228
2	University of Southern California Department of Aerospace Engineering ATTN: T. Maxworthy P. Weidman Los Angeles, CA 90007
2	University of Michigan Department of Aeronautical Engineering ATTN: W.W. Wilmarth Tech Library East Engineering Building Ann Arbor, MI 48104
1	University of California - Santa Barbara Department of Mechanical and Environmental Engineering ATTN: J.P. Vanyo Santa Barbara, CA 93106

<u>No. of Copies</u>	<u>Organization</u>
3	University of Virginia Department of Mechanical and Aerospace Engineering ATTN: H.G. Wood R.J. Ribando R. Krauss Prof. Ira Jacobson Charlottesville, VA 22904
1	University of Tennessee Department of Physics ATTN: Tech Library Knoxville, TN 37916
1	University of Washington Department of Mechanical Engineering ATTN: Tech Library Seattle, WA 98105
1	University of Wyoming ATTN: D.L. Boyer University Station Laramie, WY 82071
1	University of Wisconsin - Madison Center for Mathematical Sciences ATTN: John C. Strikwerda 610 Walnut Street Madison, WI 53706
1	Woods Hole Oceanographic Institute ATTN: J.A. Whitehead Woods Hole, MA 02543
1	Virginia Polytechnic Institute and State University Department of Engineering Science and Mechanics ATTN: Tech Library Blacksburg, VA 24061
1	Fluid Dynamics International ATTN: Dr. Simon Rosenblat 1600 Orrington Avenue Suite 505 Evanston, IL 60201
1	Rockwell International Science Center ATTN: Dr. S. Chakravarthy 1049 Camino Dos Rios P.O. Box 1085 Thousand Oaks, CA 91360
1	ICASE ATTN: Prof. Philip Hall, Mail Stop 132-C NASA Langley Research Center Hampton, VA 23665

<u>No. of Copies</u>	<u>Organization</u>
1	Mr. Harold Vaughn 7709 Gladden N.E. Albuquerque, NM 87110
	<u>Aberdeen Proving Ground</u> Commander, CRDEC, AMCCOM ATTN: SMCCR-MU, Mr. W. Dee ATTN: SMCCR-RSP-A, Mr. M. Miller

## USER EVALUATION SHEET/CHANGE OF ADDRESS

This Laboratory undertakes a continuing effort to improve the quality of the reports it publishes. Your comments/answers to the items/questions below will aid us in our efforts.

1. BRL Report Number BRL-TR-3096 Date of Report APRIL 1990
2. Date Report Received \_\_\_\_\_
3. Does this report satisfy a need? (Comment on purpose, related project, or other area of interest for which the report will be used.) \_\_\_\_\_  
\_\_\_\_\_  
\_\_\_\_\_
4. Specifically, how is the report being used? (Information source, design data, procedure, source of ideas, etc.) \_\_\_\_\_  
\_\_\_\_\_  
\_\_\_\_\_
5. Has the information in this report led to any quantitative savings as far as man-hours or dollars saved, operating costs avoided, or efficiencies achieved, etc? If so, please elaborate. \_\_\_\_\_  
\_\_\_\_\_  
\_\_\_\_\_
6. General Comments. What do you think should be changed to improve future reports? (Indicate changes to organization, technical content, format, etc.) \_\_\_\_\_  
\_\_\_\_\_  
\_\_\_\_\_  
\_\_\_\_\_

### CURRENT ADDRESS

\_\_\_\_\_  
Name

\_\_\_\_\_  
Organization

\_\_\_\_\_  
Address

\_\_\_\_\_  
City, State, Zip Code

7. If indicating a Change of Address or Address Correction, please provide the New or Correct Address in Block 6 above and the Old or Incorrect address below.

### OLD ADDRESS

\_\_\_\_\_  
Name

\_\_\_\_\_  
Organization

\_\_\_\_\_  
Address

\_\_\_\_\_  
City, State, Zip Code

(Remove this sheet, fold as indicated, staple or tape closed, and mail.)

-----FOLD HERE-----

**DEPARTMENT OF THE ARMY**

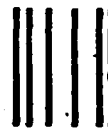
Director

U.S. Army Ballistic Research Laboratory

ATTN: SLCBR-DD-T

Aberdeen Proving Ground, MD 21005-5066

**OFFICIAL BUSINESS**



NO POSTAGE  
NECESSARY  
IF MAILED  
IN THE  
UNITED STATES

**BUSINESS REPLY MAIL**

FIRST CLASS PERMIT No 0001, APG, MD

POSTAGE WILL BE PAID BY ADDRESSEE

Director

U.S. Army Ballistic Research Laboratory

ATTN: SLCBR-DD-T

Aberdeen Proving Ground, MD 21005-9989



-----FOLD HERE-----